JOURNAL OF APPLIED ELECTROCHEMISTRY 23 (1993) 873–886

Analysis of flow-through porous electrode cell with homogeneous chemical reactions: application to bromide oxidation in brine solutions

JIAN. QI*, R. F. SAVINELL‡

Department of Chemical Engineering, Case Western Reserve University, Cleveland, Ohio 44106, USA

Received 26 April 1992; revised 8 January 1993

Electrochemical generation of elemental bromine from bromide-containing brine solutions using a flow-through porous electrode system was modelled and studied. Bromine yield was undermined by the homogeneous reactions taking place in the liquid phase which converted bromine back to bromide as well as other undesirable compounds. The effects of these reactions were characterized and accounted for in a mathematical description of a flow-through porous electrode system. The resulting model was used to analyse and estimate the effects of these reactions on the cell size and the current efficiency. Experimental data obtained support the model predictions.

Nomenclature

Symbols

a	electrochemically active surface area per unit volume of electrode (cm^{-1})
B	width of flow-through electrode (cm)
C_i	concentration of species i (M)
C^0_{Br}	total Br (in various valence states) content in analyte (M)
C_{Br^-}	bromide concentration (M)
$C^1_{Br^-}, C^2_{Br^-}$	anode inlet and outlet bromide concentrations (M)
C_{BrCl}	BrCl concentration (M)
C^1_{BrCl}, C^2_{BrCl}	anode inlet and outlet BrCl concentrations (M)
$C_{BrCl_2^-}$	$BrCl_2^-$ concentration (M)
C_{Br_2}	bromine concentration (M)
$C_{Br_2Cl^-}$	Br_2Cl^- concentration (M)
$C_{Br_3^-}$	Br_3^- concentration (M)
C_{Cl^-}	chloride concentration (M)
C_{Cl_2}	aqueous chlorine concentration (M)
$C_{Cl_3^-}$	Cl_3^- concentration (M)
C_{H^+}	proton concentration (M)
$C^1_{H^+}$	anode outlet proton concentration (M)
C_{HBrO}	HBrO concentration (M)
C^1_{HBrO}	anode inlet HBrO concentration (M)
C_{HClO}	HClO concentration (M)
C^1_{HClO}	anode inlet H_{ClO} concentration (M)
D_i	sum of diffusion and dispersion coefficients of species i ($cm^2\,s^{-1}$)
F	Faraday's constant (96 485 $C\,mol^{-1}$)
f	bromide conversion
h_1, h_2, h_3	dimensionless terms representing, respectively, the effects contributed by incomplete chlorination, hydrolysis, and formation of BrCl (Equations 16–18)
I	total cell current (mA)
I_{O_2}	water oxidation current (mA)
i_i	current density of electrochemical reaction of species i ($mA\,cm^{-2}$)
i_{Br^-}	bromide oxidation current density ($mA\,cm^{-2}$)
i_{Cl^-}	chloride oxidation current density ($mA\,cm^{-2}$)
i_{O_2}	water oxidation current density ($mA\,cm^{-2}$)
K_1	equilibrium constant of Reaction R1, $= \dfrac{(C_{Cl^-})^2 C_{Br_2}}{C_{Cl_2}(C_{Br^-})^2}$
K_2	equilibrium constant of Reaction R2, $= \dfrac{C_{HBrO} C_{H^+} C_{Br^-}}{C_{Br_2}}$
K_3	equilibrium constant of Reaction R3, $= \dfrac{C_{BrCl} C_{Br^-}}{C_{Br_2} C_{Cl^-}}$
K_4	equilibrium constant of Reaction R4, $= \dfrac{C_{BrCl_2^-}}{C_{BrCl} C_{Cl^-}}$
K_5	equilibrium constant of Reaction R5, $= \dfrac{C_{Br_2Cl^-}}{C_{Br_2} C_{Cl^-}}$
K_6	equilibrium constant of Reaction R6, $= \dfrac{C_{Br_3^-}}{C_{Br^-} C_{Br_2}}$

* Present address: Occidental Chemical Corporation, 2801 Long Road, Grand Island, NY 14072, USA
‡ To whom correspondence should be addressed

0021-891X

K_7 equilibrium constant of Reaction R7, $= \frac{C_{HClO} C_{H^+} C_{Cl^-}}{C_{Cl_2}}$

K_8 equilibrium constant of Reaction R8, $= \frac{C_{Cl_3^-}}{C_{Cl^-} C_{Cl_2}}$

K_9 equilibrium constant of Reaction R9, $= \frac{C_{Br_2} C_{Cl_2}}{C_{BrCl}}$

k mass transfer coefficient or first order reaction constant for bromide ($cm\,s^{-1}$)

L electrode length (cm)

Lr ratio of electrode length considering homogeneous reactions to electrode length without homogeneous reactions

N_i superficial vector flux of species i ($mmol\,s^{-1}\,cm^{-2}$)

n number of electrons transferred when one species i is formed or depleted

$(r_i)_j$ rate of homogeneous chemical reaction j that generates species i, negative when i is consumed ($mmol\,s^{-1}\,cm^{-3}$)

$(r_{Br^-})_1$ rate of bromide depletion by Reaction R1 ($mmol\,s^{-1}\,cm^{-3}$)

$(r_{Br^-})_2$ rate of bromide generation by Reaction R2 ($mmol\,s^{-1}\,cm^{-3}$)

$(r_{Br^-})_3$ rate of bromide generation by Reaction R3 ($mmol\,s^{-1}\,cm^{-3}$)

$(r_{BrCl})_3$ rate of BrCl generation by Reaction R3 ($mmol\,s^{-1}\,cm^{-3}$)

$(r_{BrCl})_4$ rate of BrCl depletion by Reaction R4 ($mmol\,s^{-1}\,cm^{-3}$)

$(r_{BrCl})_9$ rate of BrCl depletion by Reaction R9 ($mmol\,s^{-1}\,cm^{-3}$)

$(r_{BrCl_2^-})_4$ rate of $BrCl_2^-$ generation by Reaction R4 ($mmol\,s^{-1}\,cm^{-3}$)

$(r_{Cl_2})_1$ rate of chlorine depletion by Reaction R1 ($mmol\,s^{-1}\,cm^{-3}$)

$(r_{Cl_2})_7$ rate of chlorine depletion by Reaction R7 ($mmol\,s^{-1}\,cm^{-3}$)

$(r_{Cl_2})_8$ rate of chlorine depeletion by Reaction R8 ($mmol\,s^{-1}\,cm^{-3}$)

$(r_{Cl_2})_9$ rate of chlorine generation by Reaction R9 ($mmol\,s^{-1}\,cm^{-3}$)

$(r_{Cl_3^-})_8$ rate of Cl_3^- generation by Reaction R8 ($mmol\,s^{-1}\,cm^{-3}$)

$(r_{HBrO})_2$ rate of HBrO generation by Reaction R2 ($mmol\,s^{-1}\,cm^{-3}$)

$(r_{HClO})_7$ rate of HClO generation by Reaction R7 ($mmol\,s^{-1}\,cm^{-3}$)

S porous electrode channel thickness (cm)

u_i mobility of species i ($mmol\,cm^{-2}\,J^{-1}\,s^{-1}$)

$\boldsymbol{v}$ velocity vector ($cm\,s^{-1}$)

v_0 superficial flow velocity ($cm\,s^{-1}$)

v_y superficial flow velocity in y direction ($cm\,s^{-1}$)

x electrode dimension in current flow direction (cm)

y electrode dimension in electrolyte flow direction (cm)

z electrode dimension perpendicular to x and y (cm)

z_i valence of species i

Greek symbols

ϵ void fraction of porous electrode

ψ molar concentration of BrCl as a function of bromide concentration

ϕ_2 electrostatic potential in liquid phase (V)

φ local current efficiency

Φ overall current efficiency

Φ_{est} current efficiency estimated from theory

Φ_{exp} current efficiency obtained from experiments

Superscripts

0 total
1 inlet
2 outlet

Subscripts

i species i
j reaction j

1. Introduction

Commercial bromine manufacture from bromide-containing brine is generally based on methods of brine chlorination where bromide is oxidized by chlorine to bromine which can be subsequently stripped out, using air or steam, from the brine solution [1–3]. However, it is well known that bromine generation via bromide oxidation can also be achieved electrochemically. The electrochemical route appears to be advantageous because the sodium chloride in brine solutions offers a natural supporting electrolyte and bromide oxidation can be effected at a potential of 1.09 V vs SCE; this is 0.27 V lower than the potential for chloride oxidation (1.36 V). The lower oxidation potential should lead to less energy consumption than for generation of equivalent chlorine. Additional advantages of the electrochemical process are that the electrochemical method eliminates the intermediate processes such as chlorine transportation and handling and thus offers a less hazardous and much cleaner technology. Moreover, because the electrochemical cell stacks are often movable and can be readily transported to different locations, on-site recovery of byproduct bromide generated by bromine users becomes possible. The on-site recovery of bromine alleviates bromine transportation and the consequent benefits may be considerable. Another notable feature of the electrochemical

process is its flexibility in terms of production capacity, which can be adjusted by simply assembling a different number of cells and/or stacks without altering the single cell design.

Natural brine solutions often contain impurities such as ammonium, iodide and sulphur compounds and their oxidation liberates protons and acidifies the brine stream. This, plus the unstripped chlorine and bromine as well as other compounds of the two, often increases the corrosivity of the spent brine, which must be specially neutralized or treated before disposal. In an electrochemical process, it is possible to feed a low pH, spent brine to the cathode so that the oxidizing species is reduced and the solution neutralized by water reduction at the cathode. When proper configuration and control are implemented, the corrosivity of the spent brine is minimized. This additional environmental benefit should not be overlooked since chemically treating the corrosive brine solution is very costly. Early research on developing the electrochemical technology encountered several difficulties, one of them being low current density owing to the dilute bromide concentration in natural brine solutions. The low current efficiency achieved (reported was less than 70% [1]) further disfavoured the direct electrochemical approach.

The problem of low current density may be overcome by using porous electrodes which offer large reactive surface area within a compact volume. A flow-through cell configuration of porous electrodes also greatly enhances the mass transfer coefficient. The theory and applications of flow-through electrode cells have been discussed extensively in numerous publications (e.g. [4–7]). In this work, a cell system consisting of graphite felt electrodes placed in two channels divided by a microporous polymer membrane was evaluated for bromine production. A bromide-containing brine solution was fed into the anode compartment, whereas a bromide-depleted stream of brine was passed through the cathode compartment. The direction of the electric current supplied was perpendicular to the electrolyte flow. (See Fig. 1). At the anode, bromide was oxidized to bromine, while water and proton reduction took place at the cathode. If the anode potential is sufficiently positive, chlorine and oxygen are also generated. Despite the fact that the *in situ* generated chlorine oxidizes bromide to bromine almost instantaneously, the reaction is not irreversible or 100% complete. As a result, there is always a small loss in current efficiency due to the unreacted chlorine. Oxygen generation not only reduces current efficiency but also erodes the graphite anode and should be minimized.

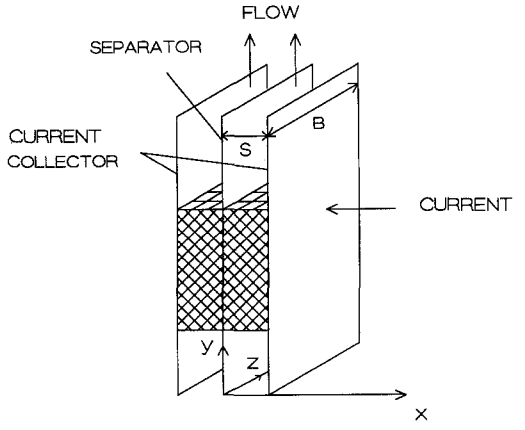

Fig. 1. Schematic diagram of a flow-through porous electrode cell.

A substantial loss of bromine yield may occur as a result of several liquid phase homogeneous reactions involving formation of BrCl, via which bromine molecules are decomposed and bromide ions are regenerated. The bromine yield can be further lowered by bromine hydrolysis to produce Br-containing species that are difficult to recover. The extent to which these homogeneous reactions affect the cell current efficiency, as well as the cell size required for a large scale bromine production, needs to be understood before a feasible electrochemical bromine process can be developed. In this paper, a process model elucidating the effects of these reactions on bromine production has been developed. Based on the model, the cell performance was evaluated under various operating conditions. Experiments were then carried out to verify the model predictions.

2. Theoretical model

2.1. Mass balance

The mass balance for a porous electrode system, adopting the treatment and the nomenclature of Newman and Tiedemann [7], can be written as

$$\nabla \cdot \boldsymbol{N}_i = \frac{a}{nF} i_i + \epsilon \sum_j (r_i)_j \tag{1}$$

where the superficial vector flux, $\boldsymbol{N}_i$, based on the combined area of solid and void can be expressed as

$$\boldsymbol{N}_i = -\epsilon D_i \nabla C_i - z_i u_i F \epsilon C_i \nabla \phi_2 + \boldsymbol{v} C_i \tag{2}$$

where the terms herein are specified in the listed nomenclature.

Referring to Fig. 1, since there is neither a net flow of current nor a flow of fluid in the z-direction, their variations along that direction are statistically zero. Therefore, all the partial derivatives with respect to z are zero if quantities averaged over z are used. Other assumptions include the following: the electrolyte flow driven by pressure difference through the microporous membrane separator is negligible; the longitudinal diffusion term can be ignored since it is much smaller than convection; the liquid phase electrostatic potential gradient in the y-direction is small. Equations 1 and 2 now can be simplified to

$$-\epsilon D_i \frac{\partial^2 C_i}{\partial x^2} - z_i u_i F \epsilon C_i \frac{\partial^2 \phi_2}{\partial x^2} + \frac{\partial (v_y C_i)}{\partial y} = \frac{a}{nF} i_i + \epsilon \sum_j (r_i)_j \tag{3}$$

Integrating with respect to x yields

$$\left[-\epsilon D_i \frac{\partial C_i}{\partial x} - z_i u_i F \epsilon C_i \frac{\partial \phi_2}{\partial x}\right]_0^S + \frac{\partial (v_y C_i)}{\partial y} S = S \frac{a}{nF} i_i + \epsilon S \sum_j (r_i)_j \quad (4)$$

In this equation quantities averaged over the x–z plane should be used. If no reaction occurs at the current collector located at $x = S$, then the net flux in the x-direction at $x = S$ must be zero. Also, for a brine solution, the current across the microporous cell separator is mainly carried by Na^+ and Cl^- because of their high concentrations, and the inter-compartmental transport of species other than Na^+ and Cl^- is attributed to the diffusion across the separator, which is usually negligible compared to electrolysis or homogeneous reactions terms. Thus the bracketed term of Equation 4 disappears. With the assumption of flow continuity (this may not be true if a significant amount of gas bubbles are present in the flow channel as in the catholyte where large amounts of hydrogen evolution take place) Equation 4 is reduced to

$$v_0 \frac{\partial C_i}{\partial y} = \frac{a}{nF} i_i + \epsilon \sum_j (r_i)_j \quad (5)$$

in which v_0 is the averaged v_y, i.e. the superficial velocity. This equation should be applicable to all species for which inter-compartmental transport (by migration or diffusion) is negligible. Note that C_i in Equation 5 represents the concentration of species i averaged over the cross section of the flow channel.

2.2. Mass balance of Br^-

Electrochemical oxidation of bromide is often accompanied by chlorine generation because of the large overpotential usually needed for achieving bromide oxidation current at low concentrations. The *in situ* generated chlorine reacts rapidly with bromide in the electrolyte:

$$2Br^- + Cl_2(aq) \rightleftharpoons Br_2(aq) + 2Cl^- \qquad K_1 = 3 \times 10^{10} \quad (R1)$$

But the yield of bromine is hampered by hydrolysis:

$$Br_2(aq) + H_2O \rightleftharpoons H^+ + Br^- + HBrO \qquad K_2 = 5.8 \times 10^{-9} \quad (R2)$$

as well as by formation of BrCl:

$$Br_2(aq) + Cl^- \rightleftharpoons BrCl(aq) + Br^- \qquad K_3 = 0.00012 \quad (R3)$$

Reaction R1 is believed to proceed in two steps [3]: (i) $Br^- + Cl_2(aq) \rightleftharpoons BrCl(aq) + Cl^-$ and (ii) $Br^- + BrCl(aq) \rightleftharpoons Br_2(aq) + Cl^-$. Since the overall reaction, R1, has already been written, only one of these reactions needs to be given here. Other homogeneous reactions in a Br^-–$Br_2(aq)$–Cl^-–H_2O system that affect the above reactions are [1, 8–13]:

$$BrCl(aq) + Cl^- \rightleftharpoons BrCl_2^- \qquad K_4 = 5.3 \quad (R4)$$
$$Br_2(aq) + Cl^- \rightleftharpoons Br_2Cl^- \qquad K_5 = 1.42 \quad (R5)$$
$$Br_2(aq) + Br^- \rightleftharpoons Br_3^- \qquad K_6 = 20.2 \quad (R6)$$
$$Cl_2(aq) + H_2O \rightleftharpoons H^+ + Cl^- + HClO \qquad K_7 = 4.8 \times 10^{-4} \quad (R7)$$
$$Cl_2(aq) + Cl^- \rightleftharpoons Cl_3^- \qquad K_8 = 0.13 \quad (R8)$$
$$2BrCl(aq) \rightleftharpoons Br_2(aq) + Cl_2(aq) \qquad K_9 \quad (R9)$$

where K_1 to K_9 are the equilibrium constants based on molar concentrations.

The values for K_1, K_4, K_5, K_6, and K_8 are reported in [10] for aqueous solutions of NaCl and NaBr at 25 °C with ionic strength of 4 M, while K_3 at 25 °C is reported in [13]. For K_2 and K_7, only the values for hydrolysis in pure water (25 °C) are available [1]. It will be shown later that K_9 is not needed.

The effect of the activity of each species on the equilibrium constants is not considered here and the formation of pentabromide ion Br_5^- and the slight ionization of HBrO (only about 0.1% HBrO is ionized) have been neglected [1]. The reaction between HClO and Br^- or HBrO is also negligible. Reactions R1 to R9 occur rapidly and instantaneous attainment of equilibrium is usually assumed [3, 12]. Because Reaction R6 does not change the valence of Br^- or Br_2, it is not considered to deplete bromide or bromine, although the existence of Br^-_3 affects equilibrium involving bromide or bromine. On the other hand, Reactions R1, R2 and R3 should be accounted for in $\Sigma_j (r_i)_j$ when applying Equation 5 to Br^-:

$$v_0 \frac{dC_{Br^-}}{dy} = -\frac{a}{F} i_{Br^-} + \epsilon[-(r_{Br^-})_1 + (r_{Br^-})_2 + (r_{Br^-})_3] \quad (6)$$

A negative sign is added before i_{Br^-} since bromide is consumed by the electrolysis. A negative sign is also added to the term $(r_{Br^-})_1$ to indicate that bromide is consumed when Reaction R1 proceeds from left to right. Usually, solving Equation 9 requires knowledge of the chemical reaction rate expressions. In our approach, these reaction rates are related to the gradient of the various dissolved species in the flow direction by applying Equation 5 to each species:

$$v_0 \frac{dC_{Cl_2}}{dy} = \frac{a}{2F} i_{Cl^-} + \epsilon[-(r_{Cl_2})_1 - (r_{Cl_2})_7 - (r_{Cl_2})_8 + (r_{Cl_2})_9] \quad (7)$$

$$v_0 \frac{dC_{HBrO}}{dy} = \epsilon (r_{HBrO})_2 \quad (8)$$

$$v_0 \frac{dC_{BrCl}}{dy} = \epsilon[(r_{BrCl})_3 - (r_{BrCl})_4 - (r_{BrCl})_9] \quad (9)$$

$$v_0 \frac{dC_{BrCl_2^-}}{dy} = \epsilon (r_{BrCl_2^-})_4 \quad (10)$$

$$v_0 \frac{dC_{HClO}}{dy} = \epsilon(r_{HClO})_7 \quad (11)$$

$$v_0 \frac{dC_{Cl_3^-}}{dy} = \epsilon(r_{Cl_3^-})_8 \quad (12)$$

Note that the magnitudes of the rates are related by $2(r_{Cl_2})_1 = (r_{Br^-})_1$; $(r_{HBrO})_2 = (r_{Br^-})_2$; $(r_{BrCl})_3 = (r_{Br^-})_3$; $(r_{BrCl_2^-})_4 = (r_{BrCl})_4$; $(r_{HClO})_7 = (r_{Cl_2})_7$; $(r_{Cl_3^-})_8 = (r_{Cl_2})_8$; and $(r_{BrCl})_9 = 2(r_{Cl_2})_9$. Using these relationships to combine Equation 7 through Equation 12 results in

$$-a\frac{i_{Cl^-}}{F} + v_0\left(2\frac{dC_{Cl_2}}{dy} + \frac{dC_{HBrO}}{dy} + \frac{dC_{BrCl}}{dy} + \frac{dC_{BrCl_2^-}}{dy} + 2\frac{dC_{HClO}}{dy} + 2\frac{dC_{Cl_3^-}}{dy}\right) = \epsilon[-(r_{Br^-})_1 + (r_{Br^-})_2 + (r_{Br^-})_3] \quad (13)$$

Therefore Equation 6 becomes

$$\frac{dC_{Br^-}}{dy} = -\frac{a}{v_0}\frac{i_{Br^-} + i_{Cl^-}}{F} + 2\frac{dC_{Cl_2}}{dy} + \frac{dC_{HBrO}}{dy} + \frac{dC_{BrCl}}{dy} + \frac{dC_{BrCl_2^-}}{dy} + 2\frac{dC_{HClO}}{dy} + 2\frac{dC_{Cl_3^-}}{dy} \quad (14)$$

The void fraction shown in Equation 6 disappeared in this equation. It is noteworthy that although reaction $Br^- + BrCl \rightleftharpoons Br_2Cl^-$ also exists [9], it is only an intermediate step of Reactions R3 and R5 and can be shown not to affect the final expression of Equation 14 by similar derivations. Also, it can be shown that Equation 14 remains the same even if $Br^- + Cl_2 \rightleftharpoons BrCl + Cl^-$ is included, which is the first step of Reaction R1, since only the independent reactions matter.

Equation 14 reveals that formation of Br_2Cl^- does not affect bromide conversion. In fact, Reaction R5, similar to R6, merely forms a bromine complex and does not change the bromine valence. Therefore it only affects the bromine equilibrium. In the absence of water oxidation, $i_{Br^-} + i_{Cl^-}$ becomes the total current density.

If the concentrations of the species involved in Equation 14 are all functions of C_{Br^-} only, as will be shown later, the following manipulation is valid:

$$2\frac{dC_{Cl_2}}{dy} + \frac{dC_{HBrO}}{dy} + \frac{dC_{BrCl}}{dy} + \frac{dC_{BrCl_2^-}}{dy} + 2\frac{dC_{HClO}}{dy} + 2\frac{dC_{Cl_3^-}}{dy} = \left(2\frac{dC_{Cl_2}}{dC_{Br^-}} + 2\frac{dC_{Cl_3^-}}{dC_{Br^-}} + \frac{dC_{HBrO}}{dC_{Br^-}} + 2\frac{dC_{HClO}}{dC_{Br^-}} + \frac{dC_{BrCl}}{dC_{Br^-}} + \frac{dC_{BrCl_2^-}}{dC_{Br^-}}\right)\frac{dC_{Br^-}}{dy} \quad (15)$$

By letting

$$h_1 = -2\frac{dC_{Cl_2}}{dC_{Br^-}} - 2\frac{dC_{Cl_3^-}}{dC_{Br^-}} \quad (16)$$

$$h_2 = -\frac{dC_{HBrO}}{dC_{Br^-}} - 2\frac{dC_{HClO}}{dC_{Br^-}} \quad (17)$$

$$h_3 = -\frac{dC_{BrCl}}{dC_{Br^-}} - \frac{dC_{BrCl_2^-}}{dC_{Br^-}} \quad (18)$$

where the terms, h_1, h_2, and h_3, represent the effects of chlorination, hydration, and BrCl formation, respectively, Equation 14 can be written as

$$(1 + h_1 + h_2 + h_3)\frac{dC_{Br^-}}{dy} = -\frac{a}{v_0}\frac{i_{Br^-} + i_{Cl^-}}{F} \quad (19)$$

Note that when i_{Cl^-}, h_1, h_2, and $h_3 = 0$, Equation 19 is reduced to the conventional equation for porous electrode.

In order to solve Equation 19, h_1, h_2, and h_3 need to be first related to C_{Br^-}. In this approach, the relationship is derived using the equilibrium equations for the homogeneous reactions, because these reactions are rapid and establishment of their equilibria is usually considered virtually instantaneous. Thus, the concentrations of each species involved should be at, or at least close to, the equilibrium concentrations, especially for a process where the electrolysis step is much slower than the homogeneous reactions.

2.3. Liquid phase equilibria

If no water oxidation takes place at the anode and the change in C_{H^+} by ionization of water, HBrO, or HClO can be neglected, then, for a closed system, the following mass balance holds:

$$C_{H^+} = C^1_{H^+} + C_{HBrO} + C_{HClO} - C^1_{HBrO} - C^1_{HClO} \quad (20)$$

where superscript 1 denotes anode inlet conditions. According to Equation 20, the pH of the anolyte should decrease as bromide conversion and chlorine generation increase. Using the equilibrium equations one obtains,

$$C_{HBrO} = \frac{K_1K_2C_{Br^-}}{2(K_1K_2C_{Br^-} + K_7C_{Cl^-})} \cdot \times \left\{\left[(C^1_{H^+} - C^1_{HBrO} - C^1_{HClO})^2 + \frac{4C_{BrCl}}{K_3}\left(\frac{K_2}{C_{Cl^-}} + \frac{K_7}{K_1C_{Br^-}}\right)\right]^{1/2} - (C^1_{H^+} - C^1_{HBrO} - C^1_{HClO})\right\} \quad (21)$$

The detailed derivation of this expression is given in the Appendix. This equation suggests that bromine hydrolysis can be reduced by lowering the solution pH.

For a closed system,

$$C_{Br^-} + 2C_{Br_2} + 3C_{Br_3^-} + C_{BrCl} + C_{BrCl_2^-} + 2C_{Br_2Cl} + C_{HBrO} = C_{Br}^0 \quad (22)$$

where C_{Br}^0 is the sum of all Br in Br-containing species. After substituting C_{Br_2}, $C_{Br_3^-}$, $C_{BrCl_2^-}$, and $C_{Br_2Cl^-}$ using the expressions for K_3, K_4, K_5, and K_6, rearranging gives

$$\left[\frac{3K_6}{K_3C_{Cl^-}}(C_{Br^-})^2 + \left(\frac{2}{K_3C_{Cl^-}} + \frac{2K_5}{K_3}\right)C_{Br^-} + K_4C_{Cl^-} + 1\right]C_{BrCl} = C_{Br}^0 - C_{Br^-} - C_{HBrO} \quad (23)$$

where C_{HBrO} can be replaced by Equation 21. Usually, C_{Cl^-} and C_{Br}^0 remain unaffected by the small intercompartmental transport and are basically constant throughout the anode compartment. Therefore, Equation 23 can be solved to give C_{BrCl} as a function of C_{Br^-}, which decreases as the anolyte approaches the anode outlet. Let ψ represent the C_{BrCl} obtained from Equation 23. The expressions for h_1, h_2, and h_3 can be derived (see the Appendix for the details of the derivation):

$$h_1 = -2\frac{dC_{Cl_2}}{dC_{Br^-}} - 2\frac{dC_{Cl_3^-}}{dC_{Br^-}} = -(1 + K_8C_{Cl^-})\frac{2C_{Cl^-}}{K_1K_3C_{Br^-}}\left[\psi' - \frac{\psi}{C_{Br^-}}\right] \quad (24)$$

$$h_2 = -\frac{dC_{HBrO}}{dC_{Br^-}} - 2\frac{dC_{HClO}}{dC_{Br^-}} = -\left[1 + \frac{2K_7C_{Cl^-}}{K_1K_2C_{Br^-}}\right]\frac{dC_{HBrO}}{dC_{Br^-}} + 2\frac{K_7C_{Cl^-}C_{HBrO}}{K_1K_2(C_{Br^-})^2} \quad (25)$$

$$h_3 = -\frac{dC_{BrCl}}{dC_{Br^-}} - \frac{dC_{BrCl_2^-}}{dC_{Br^-}} = -(1 + K_4C_{Cl^-})\psi' \quad (26)$$

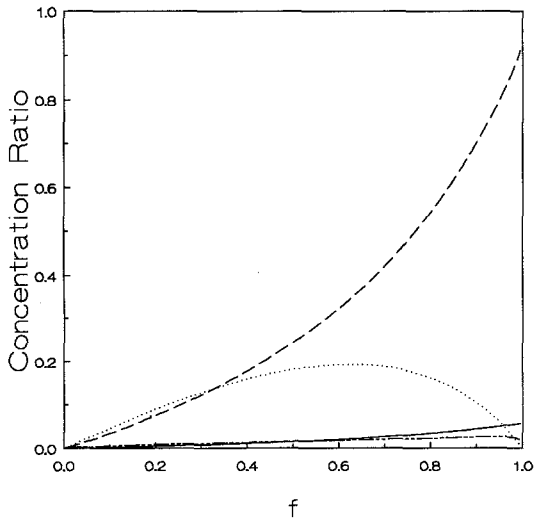

Fig. 2. Distribution of each species at various bromide conversions: $C_{Br^-}^1 = C_{Br}^0 = 0.001$ M, $C_{Cl^-} = 3$ M, $C_{H^+}^1 = 10^{-7}$ M, $C_{HBrO}^1 = C_{HClO}^1 = 0$. Legend: (——) C_{BrCl}/C_{Br}^0; (- - - -) $C_{BrCl_2^-}/C_{Br}^0$; (···) $2C_{Br_2Cl^-}/C_{Br}^0$; (— · · —) $2C_{HBrO}/C_{Br}^0$.

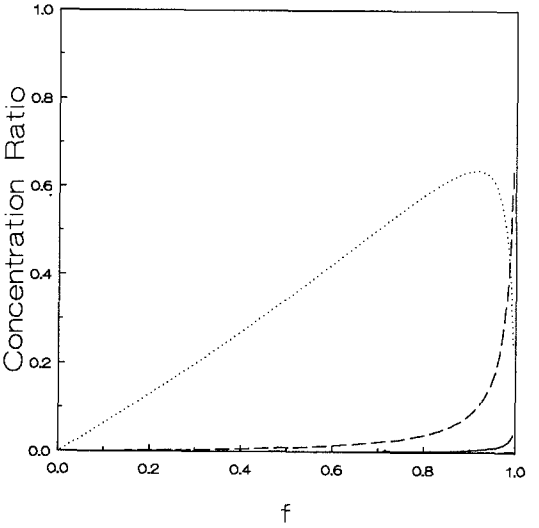

Fig. 3. Distribution of each species at various bromide conversions: $C_{Br^-}^1 = C_{Br}^0 = 0.05$ M; $C_{Cl^-} = 3$ M; $C_{H^+}^1 = 10^{-7}$ M; $C_{HBrO}^1 = C_{HClO}^1 = 0$. Legend: (——) C_{BrCl}/C_{Br}^0; (- - - -) $C_{BrCl_2^-}/C_{Br}^0$; (···) $2C_{Br_2Cl^-}/C_{Br}^0$; (— · · —) $2C_{HBrO}/C_{Br}^0$.

where ψ' is the derivative of ψ with respect to C_{Br^-}; and C_{HBrO} and dC_{HBrO}/dC_{Br^-} can be obtained from Equations 21 and 23 as functions of C_{Br^-} and ψ (which in turn, is a function of C_{Br^-}). These equations reveal that Reaction R9 does not affect bromide mass balance even though the reaction may appear to affect BrCl concentration. In fact, Reaction R9 can be obtained by combining Reactions R1 and R3 and hence K_9 can be derived from K_1 and K_3.

3. Model analysis

3.1. Significance of each reaction

To assess the relative significance of each reaction, C_{BrCl}/C_{Br}^0, $C_{BrCl_2^-}/C_{Br}^0$, $2C_{Br_2Cl^-}/C_{Br}^0$, and C_{HBrO}/C_{Br}^0 are examined at various bromide conversions using the equilibrium relationships for anolytes initially composed of NaCl and NaBr (i.e. $C_{Br}^0 = C_{Br^-}^1$). The bromide conversion is defined as

$$f = \frac{C_{Br^-}^1 - C_{Br^-}^2}{C_{Br^-}^1} \quad (27)$$

where $C_{Br^-}^2$ is the outlet bromide molar concentration. Figures 2 and 3 display the calculation results at $C_{Br}^0 = 0.001$ M and 0.05 M, respectively. An industrial bromide oxidation process is usually operated under acidic conditions and thereby the effect of HBrO is minimal. Hence, specifying $C_{H^+}^1$ at 10^{-7} M in both figures gives the upper bound of the HBrO effect.

These figures indicate that the bromine produced is mostly either in the forms of ionic complexes of Br_2 with Cl^- (i.e. Br_2Cl^-) or converted to $BrCl_2^-$ (a complex of BrCl and Cl^-) and that HBrO is appreciable only for brine with a low bromide level. Formation of $BrCl_2^-$ becomes highest at large bromide conversion. Since Br_2 is consumed and Br^- is regenerated during the formation of BrCl and HBrO (see

Reactions R2 and R3), the high percentage presence of BrCl and HBrO means that a significant amount of Br_2 generated electrochemically is converted, by the homogeneous reactions, back to Br^- and a species difficult to recover, thereby reducing the efficiency of the electrochemical process. This is true, even if 100% recovery of Br present in $BrCl/BrCl_2^-$ and HBrO can be assumed (since Cl in $BrCl/BrCl_2^-$ would still be wasted). The efficiency, however, can be improved if the Cl present in $BrCl/BrCl_2^-$ can be recovered and used to oxidize additional Br^-.

This analysis also suggests that the bromide level is critical to the feasibility of the recovery process. For example, for ocean water where bromide content is typically below 0.001 M, these effects are very pronounced and must be minimized before an efficient recovery becomes possible.

3.2. Anode size

If expressions for i_{Br^-} and i_{Cl^-} as functions of bromide concentration (or electrode position) are known, Equation 19 can be integrated numerically to give the concentration profile of bromide and other species along the anolyte flow channel. Using Equation 23, ψ' can be shown to be negative, indicating that BrCl concentration increases with bromide conversion. A larger bromide conversion can be achieved by increasing the anode length. Bromide oxidation controlled by mass transfer of bromide ions can be written as

$$i_{Br^-} = FkC_{Br^-} \tag{28}$$

where k is the mass transfer coefficient. If the process is controlled by the surface kinetics, Equation 28 is still valid for a first order reaction if the anode potential is uniformly distributed, except that k in this case will be the reaction constant instead of the mass transfer coefficient. Because of the high chloride concentration in brine solution, i_{Cl^-} can be considered constant in the cell. Using Equation 19, one obtains

$$aLk/v_0 = -\int_{C^1_{Br^-}}^{C^2_{Br^-}} \frac{1+h_1+h_2+h_3}{C_{Br^-}+i_{Cl^-}/Fk}\,dC_{Br^-} \tag{29}$$

where L is the anode length. Since h_1, h_2, and h_3 are functions of C_{Br^-} only, the above equation can be solved for a known k to give the anode length needed for various bromide conversions.

Equation 29 clearly shows that anode length is shortened by chlorine generation current. Since $h_1 > 0$, $h_2 > 0$, and $h_3 > 0$, the term $1 + h_1 + h_2 + h_3$ is greater than unity and increases with bromide conversion. Therefore, a longer anode is required for a given bromide conversion as a result of the homogeneous reactions. The terms h_1, h_2, and h_3, can be viewed as contribution to the overall effect of the homogeneous reactions by incomplete chlorination (R1, R8), hydrolysis (R2, R7), and formation of BrCl and $BrCl_2^-$ (R3, R4), respectively. To show the relative significance of each effect, $h_1/(1+h_1+h_2+h_3)$, $h_2/(1+h_1+h_2+h_3)$, and $h_3/(1+h_1+h_2+h_3)$ against f are displayed graphically in Figs 4 and 5 for two different values of C^0_{Br}. Figure 4 reiterates that the effect of hydrolysis (h_2) is appreciable only for low C^0_{Br} at a low conversion. The contribution by h_1 is nearly zero when $f < 90\%$ (therefore, Reaction R1 can be considered irreversible, i.e. $K_1 \to \infty$ for a small f, and chlorine generated at the anode in this case is equivalent to direct generation of bromine) and rises rapidly when bromide conversion exceeds 90% and becomes most significant at even higher bromide conversion (see Fig. 4). On the other hand, Fig. 5 suggests that for high C^0_{Br}, the effects of h_1 and h_2 almost disappear and h_3 becomes dominant over almost the entire range of f.

For a case where all the homogeneous reactions can be neglected, i.e. $h_1 + h_2 + h_3 = 0$, Equation 29

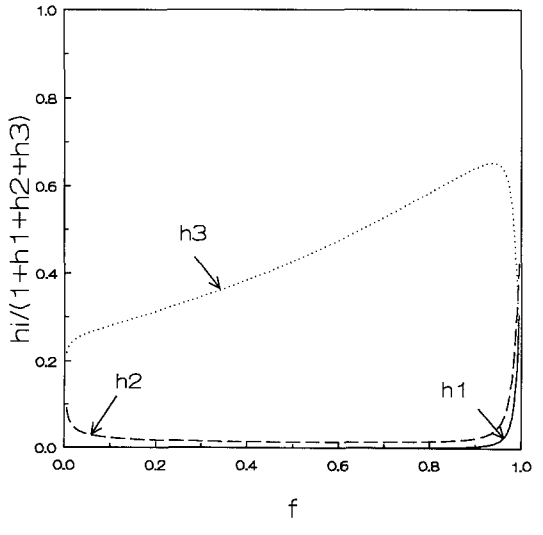

Fig. 4. Relative values of h_1, h_2, and h_3 for different bromide conversions: $C^1_{Br^-} = C^0_{Br} = 0.001$ M; $C_{Cl^-} = 3$ M; $C^1_{H^+} = 10^{-7}$ M; $C^1_{HBrO} = C^1_{HClO} = 0$.

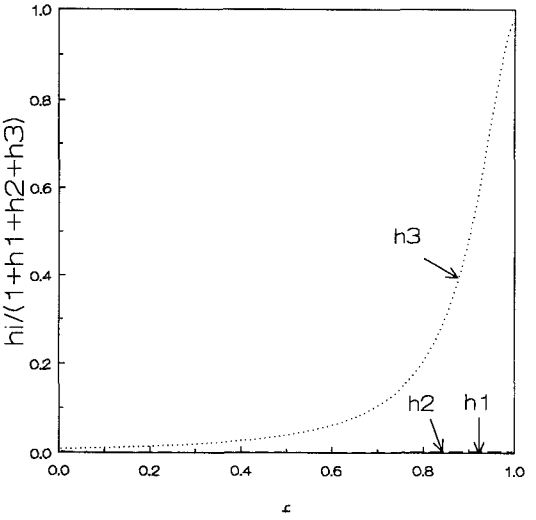

Fig. 5. Relative values of h_1, h_2, and h_3 for different bromide conversions: $C^1_{Br^-} = C^0_{Br} = 0.05$ M; $C_{Cl^-} = 3$ M; $C^1_{H^+} = 10^{-7}$ M; $C^1_{HBrO} = C^1_{HClO} = 0$.

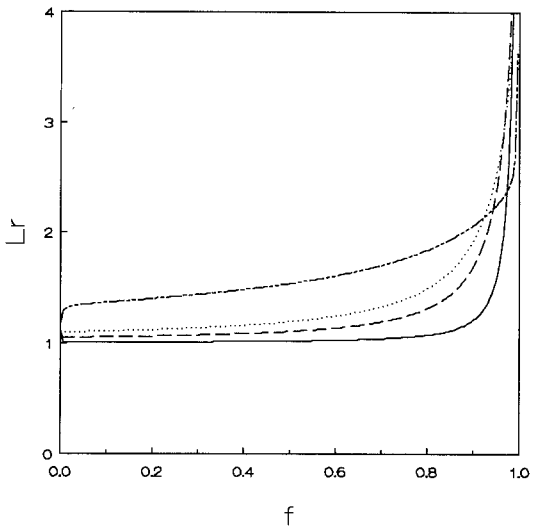

Fig. 6. Anode length ratio, Lr, required for various bromide conversions at different inlet bromide concentrations: $C^1_{Br^-} = C^0_{Br}$; $C_{Cl^-} = 3$ M; $C^1_{H^+} = 10^{-7}$ M; $C^1_{HBrO} = C^1_{HClO} = 0$. Legend, C^0_{Br}: (——) 0.05 M, (— — -) 0.01 M, (·····) 0.005 M, (— - - —) 0.001 M

reduces to

$$akL/v_0 = -\int_{C^1_{Br^-}}^{C^2_{Br^-}} \frac{1}{C_{Br^-} + i_{Cl^-}/Fk} dC_{Br^-} \qquad (30)$$

In the absence of i_{Cl^-}, the anode length for a given bromide conversion calculated from Equation 30 is independent of the inlet bromide concentration. But this is not true when the homogeneous reactions are considered. To compute the effect of the homogeneous reactions on anode length, the following is defined:

$$Lr = \frac{\text{anode length with homogeneous reactions}}{\text{anode length without homogeneous reactions}} \qquad (31)$$

where Lr is unity when the homogeneous reactions can be ignored and becomes larger when the effects of the homogeneous reactions increase. Using Equations 29 and 30 and letting $i_{Cl^-} = 0$, $C^1_{Br^-} = C^0_{Br}$, Lr at various bromide conversions are computed for several different inlet bromide concentrations. The computed results (Fig. 6) suggest that the homogeneous reaction increases the necessary anode length for a desired bromide conversion, especially when a brine containing a low level of bromide is processed. For a brine solution with a bromide level less than 0.01 M, the anode length has to be twice ($Lr > 2$) more than for a process free of the homogeneous reactions in order to achieve 90% conversion.

The characteristic that Lr increases with decrease in C^0_{Br} does not appear to be true at high bromide conversions, as shown in Fig. 6. In effect, the curve for $C^0_{Br} = 0.01$ M crosses all other curves in the region beyond 90% conversion and does not continue to rise with f as sharply as the others. This can be understood by examining Equation 23, which indicates that when $C^0_{Br} \to 0$, $C_{BrCl} \to C^0_{Br} f/(K_4 C_{Cl^-} + 1)$ (let $C^1_{Br^-} = C^0_{Br}$ and $C_{HBrO} = 0$). This means that for a fixed f, C_{BrCl} actually decreases with decrease in C^0_{Br} in low range of C^0_{Br}.

3.3. Local current efficiency

When the anode potential is sufficiently positive, water oxidation may occur at the anode in addition to generation of bromine and chlorine. The local current efficiency based on bromide converted over a differential length of anode can be defined as

$$\varphi = -\frac{Fv_0 dC_{Br^-}}{a(i_{Br^-} + i_{Cl^-} + i_{O_2})dy} \qquad (32)$$

where the negative sign is included to yield a positive value. The numerator in this equation represents the theoretical current required for electrode length dy to electrochemically convert dC_{Br^-} amount of bromide to bromine. The denominator is the total current actually consumed over the electrode length dy. Since the produced bromine subsequently participates in the homogeneous reactions and generates other Br containing compounds, the oxidized bromide is present not only in the form of bromine but also in the forms of BrCl, $BrCl_2^-$, HBrO etc. In an industrial process, a separation scheme following the electrochemical process is required to collect bromine from Br_2Cl^-, Br_3^-, BrCl, etc. in the liquid stream. Although Br_2Cl^- and Br_3^- are readily recoverable, BrCl is more difficult to strip out. Therefore the final efficiency based on bromine yield greatly depends on the separation process and the efficiency for bromine production may be enhanced significantly by improving the downstream separation efficiency.

From Equations 19 and 32, one obtains

$$\frac{1}{\varphi} = 1 + h_1 + h_2 + h_3 - \frac{ai_{O_2}}{Fv_0}\left(\frac{dy}{dC_{Br^-}}\right) \qquad (33)$$

When there is no water oxidation, Equation 32 becomes

$$\frac{dC_{Br^-}}{dy} = -\frac{a\varphi}{v_0}\frac{i_{Br^-} + i_{Cl^-}}{F} \qquad (34)$$

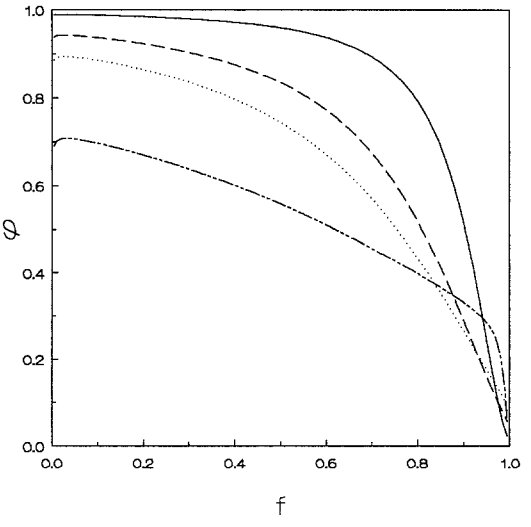

Fig. 7. Local current efficiency as a function of bromide conversion at different inlet bromide concentrations: $C^1_{Br^-} = C^0_{Br}$; $C_{Cl^-} = 3$ M; $C^1_{H^+} = 10^{-7}$ M; $C^1_{HBrO} = C^1_{HClO} = 0$. Legend: as in Fig. 6.

This equation is equivalent to Equation 29. It becomes clear that the anode length is directly associated with the local current efficiency. Improving current efficiency reduces not only the energy consumption but also decreases the necessary anode length.

Using Equation 29 and assuming no oxygen generation, the local current efficiency at various bromide conversions is plotted in Fig. 7 for inlet brine streams of different bromide concentrations. The small increase in local current efficiency with f when f is below 5% is due to the decrease in h_2. This increase is more pronounced at a lower total bromide inlet concentration. In the region of $f > 10\%$, the local current efficiency drops as the bromide conversion increases. It falls almost to zero when the bromide conversion exceeds 98%. Since higher bromide conversion is at the downstream end of the anode, the local current efficiency is lowest near the anolyte outlet. Therefore, simply increasing the electrode length to improve the bromide conversion is not only ineffective but also energy inefficient.

3.4. Cell current efficiency

The overall cell current efficiency, Φ, can be defined as

$$\Phi = \frac{\int \varphi(i_{Br^-} + i_{Cl^-} + i_{O_2})dy}{\int (i_{Br^-} + i_{Cl^-} + i_{O_2})dy} \tag{35}$$

or, after using Equation 32,

$$\Phi = -\frac{Fv_0}{a}\frac{\int dC_{Br^-}}{\int (i_{Br^-} + i_{Cl^-} + i_{O_2})dy} = Fv_0SB\frac{C^1_{Br^-} - C^2_{Br^-}}{I} \tag{36}$$

where I is the total current passing through the cell. Using Equation 32, Equation 35 can be also written as

$$\Phi = \frac{\int dC_{Br^-}}{\int (1/\varphi)dC_{Br^-}} \tag{37}$$

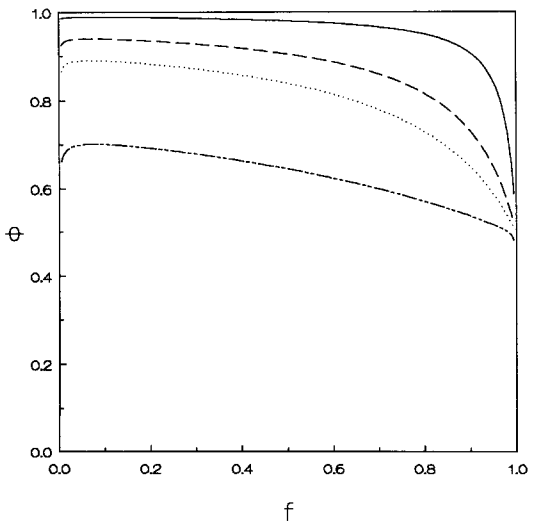

Fig. 8. Overall current efficiency for various bromide conversions at several different inlet bromide concentrations: $C^1_{Br^-} = C^0_{Br}$; $C_{Cl^-} = 3$ M; $C^1_{H^+} = 10^{-7}$ M; $C^1_{HBrO} = C^1_{HClO} = 0$. Legend: as in Fig. 6.

Replacing φ using Equation 33 and h_1 to h_3 using Equations 16 to 18 and then integrating gives

$$\left\{\Phi = -\Delta C_{Br^-}/ - \Delta C_{Br^-} + \Delta C_{BrCl} + \Delta C_{BrCl_2^-} + 2(\Delta C_{Cl_2} + \Delta C_{Cl_3^-} + \Delta C_{HClO}) + \Delta C_{HBrO} + \frac{I_{O_2}}{Fv_0SB}\right\} \tag{38}$$

where Δ denotes concentration change (outlet concentration minus inlet concentration).

Equation 38 reveals that the current efficiency is decreased by generation of the oxidized species other than bromine. Since any chlorine generation in the system consumes electricity, a net increase in its concentration translates to an extra consumption of electricity put into the system. Therefore, the denominator in Equation 38 includes the net change of Cl_2, Cl_3^-, and HClO. (Excess chlorine must be used in the conventional brine chlorination process due to the homogeneous reactions. The chlorination efficiency can also be estimated by Equation 38 without the oxygen term.) The formation of HBrO and BrCl regenerates Br^- and therefore a net increase in their concentrations also accounts for efficiency loss.

When the inlet and outlet bromide concentrations, $C^1_{Br^-}$ and $C^2_{Br^-}$, are fixed, the other concentrations can be calculated from the equilibrium relationships (see Appendix). For example, C^1_{BrCl} and C^2_{BrCl} can be obtained using $C^1_{Br^-}$ and $C^2_{Br^-}$ and Equations 21 and 23. Therefore, Equation 38 can be used for theoretical evaluation of the cell current efficiency at various bromide conversions. Figure 8 is a plot of Equation 38 for brine solutions containing several different initial bromide concentrations. The overall current efficiency again is shown to be adversely affected by decreasing inlet bromide concentration. If oxygen evolution is avoided and h_1, $h_2 = 0$, the cell current efficiency becomes

$$\Phi = \frac{-\Delta C_{Br^-}}{-\Delta C_{Br^-} + \Delta C_{BrCl} + \Delta C_{BrCl_2^-}} = \frac{-\Delta C_{Br^-}}{-\Delta C_{Br^-} + (1 + K_4C_{Cl^-})\Delta C_{BrCl}} \tag{39}$$

If a feed brine contains only Br^- (namely $C^0_{Br} = C^1_{Br}$) and no BrCl, then

$$\Phi = \frac{-\Delta C_{Br^-}}{-\Delta C_{Br^-} + (1 + K_4C_{Cl^-})C^2_{BrCl}} \tag{40}$$

Equation 23 shows that when the bromide conversion approaches 100%, i.e. $C^2_{Br^-} \to 0$, then C^2_{BrCl} approaches $C^0_{Br}/(1 + K_4C_{Cl^-})$. Consequently, the current efficiency approaches 50% and is independent of C^0_{Br} or chloride concentration.

It must be kept in mind that the treatment presented in this paper is based on the bromide conversion, which may be different from the bromine yield since the loss of elemental bromine due to such compounds as HBrO and BrCl can be significant. Nevertheless,

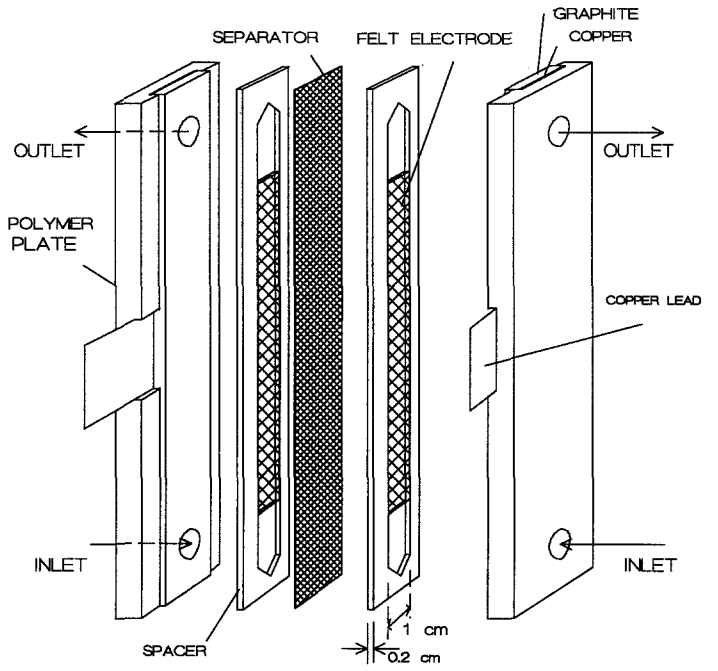

Fig. 9. A flow-through porous electrode cell assembly.

after the concentrations of these species for a given bromide conversion are calculated from the equilibrium constants as shown earlier and in the Appendix, the bromine yield can be estimated. Furthermore, BrCl may be recovered to produce additional bromine if a good separation scheme is devised. Therefore, the final yield of elemental bromine depends on the separation stages following the electrochemical process.

The effect of chloride is very straightforward in all the derived equations. The homogeneous reactions become more significant at higher chloride concentration. When no chloride is present, h_1 and h_3 are equal to zero. Since chloride concentrations generally do not vary over a wide range in the natural brine solutions, detailed discussions are omitted here.

4. Experimental verification of model

4.1. Experimental details

The assembly of a flow-through porous electrode cell used for the experimental study is illustrated schematically in Fig. 9. The cell was comprised of two identical half cells divided by a separator. Two flow channels, defined respectively by two identical Teflon spacers, housed the porous anode and cathode whose length might differ. A 0.038 cm thick microporous polyethylene membrane cell separator (Daramic, W. R. Grace & Co.) separates the anode from the cathode and prevents mixing of the anolyte and catholyte. The outer side of each spacer was pressed against the inner side of a dense graphite plate, which served as a current collector. A copper sheet was attached to the outer side of each graphite plate to provide an equipotential surface and to serve as an electrode lead to the electrical circuit. Finally, the entire cell was clamped tightly between two polymer supporting plates.

Two similar cell assemblies but with significantly different channel lengths were used. One allowed the placement of a porous electrode (in both the anode and cathode channels) of only 12 cm long, while the other could hold electrodes as long as 45 cm. The

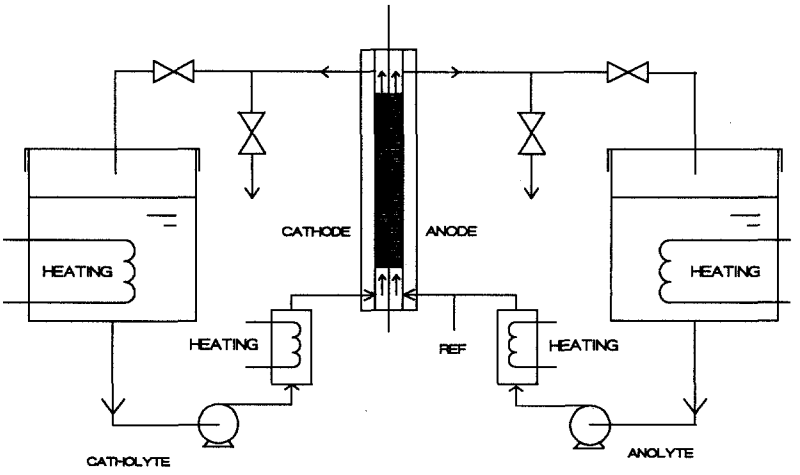

Fig. 10. Schematic diagram of the electrolyte flow system.

porous electrode used in this study was a GH 1/8 inch (3.2 mm) graphite felt (Fiber Materials, Inc.). The nominal thickness of this felt was measured to be about 0.3 cm. Because the channels defined by the Teflon spacers were machined to about 0.2 cm thick and 1 cm wide, the felt was cut into 1 cm wide and the thickness was slightly compressed when placed within the channels. The compression assured good electric contact. An RDE4 potentiostat (Pine Instruments) was used for low current experiments, whereas an Electrosynthesis Model 415 high power potentiostatic controller (Electrosynthesis, Inc.) was used when more than 400 mA was required. Since the 45 cm cell required large currents to operate, a Model TPS-2000 d.c. power supply (Topward Electric Instruments) was used to provide a current as high as 10 A for galvanostatic operations.

A schematic of the electrolyte flow system is shown in Fig. 10, where the reference electrode probe was situated at the anode inlet. The reference electrode system consisted of an SCE electrode held in an electrode reservoir filled with the anolyte solution. Both the anolyte and the catholyte were maintained at a constant temperature of 80 °C within the cell by heating the sumps and the electrolyte feed lines. (Industrial bromide recovery by chlorination generally is operated at 80 °C or above.) In addition, the entire cell was covered with insulation material to reduce heat dissipation so that temperature differences between inlet and outlet streams were minimal (< 3 °C). For the 45 cm cell, mild heating was provided to the cell through heating tapes wrapped around the cell.

The experimental current efficiency was obtained by measuring the cell current while the inlet and outlet anolyte streams were sampled for determination of bromide concentration. The current efficiency was then calculated using Equation 36. In all the experimental runs, the solution pH was adjusted below 4 to minimize bromine hydrolysis. The anolyte outlet was constantly checked to ensure that no oxygen gas bubbles were generated. In addition, polarization curves of sodium sulphate electrolyte were run using the same electrode to identify the onset potential of water oxidation so that the anode potential was controlled below that potential.

The concentration of bromide was determined based on the hypochlorite oxidation method given in [1]. The method is a well established titration method and is accurate for determination of traces of bromide in the presence of high concentration of chloride. Because bromine was found to interfere with the accuracy of this method, sample aliquots that contained bromine were first crystallized by evaporation under a mild temperature to expel the bromine before analysis. This method gave an accuracy greater than 98% when used to analyze standard samples with various concentration ratios of Br/Br^-. The standards were prepared by dissolving known quantities of NaBr and liquid bromine in water or a NaCl solution. The pH of the solution was adjusted with HCl to below 4. The total amount of dissolved bromine and BrCl could be titrated iodimetrically.

The size of sample aliquot used for each bromide analysis depended on its concentration, i.e. large aliquots for low concentration samples. Usually two or three titrations were made and an average was taken. The difference among the titrations generally was less than 1%.

4.2. Experimental results against model predictions

Experimentally, it is difficult to measure the local current efficiency since this requires well defined differential electrode dimension, sensitive measurements of current, and extremely accurate analytical method of bromide ions. Nonetheless, for a finite bromide conversion Equation 38 can be used to give an averaged local current efficiency (i.e. the cell current efficiency). When the outlet bromide concentration approaches the inlet concentration, the conversion approaches zero and the cell current efficiency approaches the local current efficiency. Therefore, the local current efficiency at various bromide conversions can be approximated by the cell efficiency measured over a small conversion but with various compositions of Br^-, Br_2, BrCl etc.

To obtain an anolyte inlet stream with such a feature, the anolyte outlet stream was recirculated back to the anolyte sump during electrolysis. Consequently, if a brine solution initially contains only

Table 1. Current efficiencies obtained at a constant anode potential (1.10 V vs SCE) in an anolyte recirculation experiment

Run	*Time/min*	*I/mA*	*Outlet pH*	$C^1_{Br^-}$/M	$C^2_{Br^-}$/M	Φ_{exp}	Φ_{est}
1	0	–	2.5	0.0500	–	–	–
	10	190	–	0.0414	0.0325	0.98	0.982
	70	146	–	0.0111	0.0063	0.69	0.734
	100	95	–	0.00368	0.00194	0.38	0.267
	160	50	1.8	0.00042	0.00034	0.03	0.030

$v_0 = 1.08\,cm\,s^{-1}$; Φ_{est} is calculated using $C_{Cl^-} = 3$ M, $C^1_{H^+} = 10^{-3}$ M, $C^0_{Br} = 0.05$ M.
Anolyte initial condition: 3 M NaCl/0.05 M NaBr/0.001 M HCl (pH 2.5), 200 ml.
Catholyte initial conditions: 3 M NaCl/0.03 M HCl, 200 ml.
Anode: $L = 2$ cm, $B = 1$ cm, $S = 0.2$ cm.
Cathode: $L = 10$ cm, $B = 1$ cm, $S = 0.2$ cm.
Temp. = 80 °C.

Table 2. Overall experimental current efficiencies compared with the theoretically estimated values

Run	$v_0/cm\,s^{-1}$	*I/mA*	$C^1_{Br^-}/M$	$C^2_{Br^-}/M$	*f*	Φ_{exp}	Φ_{est}
2	1.08	90	0.00473	0.00135	0.71	0.78	0.770
	1.08	90	0.00473	0.00155	0.67	0.74	0.787
3	1.08	86	0.00511	0.00182	0.64	0.80	0.807
	1.08	70	0.00511	0.00223	0.55	0.84	0.831
4	1.08	500	0.0500	0.0280	0.44	0.92	0.983
	1.08	500	0.0500	0.0275	0.45	0.94	0.982
5	1.08	300	0.0495	0.0360	0.27	0.94	0.987
	0.44	160	0.0495	0.0322	0.35	0.92	0.985

Single pass of anolyte. Anode potential < 1.10 V vs SCE.
Anolyte inlet stream: NaBr/3 M NaCl/0.001 M HCl. $C^0_{Br} = C^1_{Br^-}$.
Other conditions were the same as in Table 1.

NaBr, the inlet stream will contain different amounts of bromide and bromine as well as other bromine–chlorine species after a number of passes or a period of recirculation. In the experiments, the anolyte sump was closed to the atmosphere so that little bromine could escape to the atmosphere and the entire system was considered closed. Both the anolyte inlet and outlet streams of the cell were periodically sampled for bromide ion determinations while the cell current was recorded. The difference between the initial bromide concentration and the measured inlet concentration gave the bromide conversion at which the anolyte entered the cell. Since it is indicated in Fig. 7 that the local current efficiency should drop substantially in the range of high bromide conversion and will eventually drop to zero when the conversion is 100%, the current efficiency measured in a recirculating experiment should decrease as the recirculating time progresses. Indeed, such a trend has been observed (Table 1). Predictions from Equation 38 are listed in Table 1 to compare with the experimental results. Clearly, the values are in good agreement. It should also be pointed out that the pH of the anolyte dropped as predicted by Equation 20. In the model calculations, the equilibrium constants at 80 °C and in concentrated brine solutions should be used. Unfortunately, these values are not available in the literature. Instead, the values at 25 °C given earlier are used as an approximation.

Several additional experiments were run in which the anolyte inlet stream contained bromide but no bromine and was passed through the cell only once. The data obtained at several different anode inlet bromide concentrations for various conversions are presented in Table 2. As can be seen, the measured values agree closely with predictions of Equation 38.

To demonstrate the validity of model calculations applied to natural brine solutions, experiments

Table 3. Overall current efficiencies obtained using natural brine solutions

Run	ϕ_a/V *vs SCE*	$v_0/cm\,s^{-1}$	*I/mA*	$C^1_{Br^-}/M$	$C^2_{Br^-}/M$	*f*	Φ_{exp}	Φ_{est}
G1	0.95	0.99	137	0.0676	0.0608	0.10	0.95	0.985
	1.00	0.99	196	0.0676	0.0577	0.15	0.97	0.984
	1.05	0.99	265	0.0676	0.0544	0.20	0.95	0.983
G2	0.95	0.77	240	0.0714	0.0556	0.22	0.98	0.984
	1.00	0.75	403	0.0714	0.0449	0.37	0.95	0.979
	1.05	0.75	538	0.0714	0.0365	0.49	0.94	0.974
G3	1.17	0.63	860	0.0714	0.0060	0.91	0.92	0.865
	1.16	0.67	850	0.0714	0.0093	0.87	0.95	0.905
	1.14	1.53	1820	0.0714	0.0119	0.83	0.97	0.923
G4	0.95	1.04	500	0.0665	0.0426	0.36	0.96	0.978
	1.02	0.75	750	0.0665	0.0195	0.71	0.91	0.951
	1.09	0.41	750	0.0665	0.0012	0.98	0.69	0.674
	1.25	0.81	1820	0.0665	0.0009	0.99	0.56	0.643
	1.20	1.65	2400	0.0665	0.0034	0.95	0.84	0.802

Φ_{est} is calculated using $C_{Cl^-} = 5$ M, $C^1_{Br^-} = C^0_{Br}$, $C^1_{H^+} = 10^{-2}$ M.
Anode: $L = 11$ cm, $B = 1$ cm, $S = 0.2$ cm.
Cathode: $L = 10$ cm, $B = 1$ cm, $S = 0.2$ cm.
Temp. = 80 °C. Runs G3 and G4 were run galvanostatically. The others were run potentiostatically. The brine solutions had a density of 1.2 g cm^{-3} and contained about 5.5 M chloride. pH < 2.
Other components in the brine: 70 000 p.p.m. Na^+, 30 000–40 000 p.p.m. Ca^{2+}, 3000 p.p.m. Mg^{2+}, 2000 p.p.m. Sr^{2+}, 1300 boron, 120 NH^+, 75 p.p.m. sulphate, 60 p.p.m. phosphate, 20 p.p.m. barium, 10 p.p.m. manganous, 5–10 p.p.m. H_2S, 4–5 p.p.m. I^-.

Table 4. Experimental results using a tail brine from a chlorine process as the anolyte inlet

Run	Φ_a/V *vs SCE*	$v_0/cm\,s^{-1}$	*I/mA*	$C^2_{Br^-}/M$	*f*	Φ_{exp}	Φ_{est}
GT1	0.95	3.15	22	0.00160	0.13	0.67	0.716
	1.00	3.10	54	0.00120	0.37	0.71	0.681
	1.00	1.85	55	0.00080	0.56	0.68	0.636
GT2	0.95	0.43	17	0.00054	0.71	0.63	0.599
	1.00	0.40	23	0.00033	0.82	0.51	0.564
	1.03	1.15	63	0.00029	0.84	0.55	0.556
	1.00	0.43	34	0.00011	0.94	0.42	0.519

The tail brine contained a small amount of bromine due to incomplete stripping in the chlorination process. pH 0.3, $C_{Cl^-} = 5$ M. Total Br content was analysed to be 0.001 91 M and the analysis after crystallization gave 0.001 84 M of bromide. Other components were essentially the same as the raw brine except that most of the oxidizable species had already been oxidized in the chlorination process. Experimental conditions were the same as in Table 3. Φ_{est} is calculated using $C_{Cl^-} = 5$ M, $C^0_{Br} = 0.00191$ M, $C^1_{Br^-} = 0.00184$ M, $C^1_{H^+} = 10^{-2}$ M.

were conducted using raw natural brine solutions (provided by Great Lakes Chemical Corporation, El Dorado, Arkansas). The overall current efficiency obtained in these single-pass experiments is given in Table 3. Similar experiments were also conducted using a tail brine solution discharged from a chlorination process at Great Lakes Chemical Corporation as the feed to the cell. (The tail brine was a brine whose bromide had largely been recovered by the chlorine and steam stripping process.) The results are given in Table 4. During the experiments shown in Table 3, a small amount of oxygen evolution was observed when the anode potential was above 1.25 V vs SCE. The oxygen generation rate was roughly estimated to be below 50 mA by measuring the volume of the bubbles in the anolyte outlet stream. Since the cell current in those experiments was quite large, the error introduced by neglecting the generation of the oxygen was small.

The experimental results given in Tables 3 and 4 again agree with the theoretical predictions, although slight discrepancies from theoretical estimations are observed for some of the experimental data. The natural raw brine contained ammonia and a small amount of other oxidizable species which could react under certain potentials to lower current efficiency. In addition, experimental error also contributes to the difference observed at low bromide conversions since at low concentration and/or cell current, the calculation of experimental current efficiency is sensitive to the measurements of both current and concentrations. At a small cell current, even a trivial amount of oxidation of ammonia and water or other oxidizable species in the brine solutions contributes appreciably to the error in current efficiency. The theoretical values reported also contain error due to the unknown temperature effects on the equilibrium constants.

To further substantiate Equation 38, which suggests that the current efficiency is indeed independent of the anode dimension in the absence of water oxidation, current efficiency was measured using the 45 cm cell. The anode length in this cell was 45 cm, but the width and thickness were kept as before. The experimental values, presented in Table 5, again agree with the model predictions.

5. Conclusions

Electrochemical production from brine solutions has been analysed to account for the effects of liquid phase homogeneous chemical reactions. Since these reactions are considered instantaneous, the chemical reaction rates were expressed in terms of the known chemical equilibria and were incorporated into the mass balance equations. The final model allowed

Table 5. Experimental data obtained using a 45 cm long cell showing good agreement between the model estimates and the experimental measurements

Run	$v_0/cm\,s^{-1}$	*I/A*	$C^1_{Br^-}/M$	$C^2_{Br^-}/M$	*f*	Φ_{exp}	Φ_{est}
L1	6.5	6.0	0.0706	0.0253	0.64	0.96	0.96
L2	5.2	6.0	0.0706	0.0169	0.76	0.91	0.94
L3	6.6	6.0	0.0706	0.0268	0.62	0.93	0.96
L4	3.7	7.0	0.0637	0.0009	0.99	0.64	0.64
L5	4.7	6.8	0.0637	0.0025	0.96	0.82	0.78
L6	3.5	7.5	0.0705	0.0003	0.996	0.63	0.56
L7	4.7	6.8	0.0705	0.0034	0.95	0.90	0.81

Φ_{est} is calculated using $C_{Cl^-} = 5$ M, $C^1_{H^+} = 10^{-3}$ M, $C^0_{Br} = C^1_{Br^-}$.
Anolyte contains 5 M NaCl and 0.001 M NaBr.
Catholyte contains 5 M NaCl and 0.03 M HCl.
Anode: $L = 45$ cm, $B = 1$ cm, $S = 0.2$ cm.
Cathode: $L = 45$ cm, $B = 1$ cm, $S = 0.2$ cm.
Temp. = 80 °C; The anode potential is below 1.15 V vs SCE for all runs.

quantitative characterization of the effects of these homogeneous reactions on current efficiency and the electrode utilization. Experimental results have substantiated the model predictions.

It is not uncommon that an electrochemical process is accompanied by rapid homogeneous chemical reactions with rates that are difficult to measure or estimate. However, very frequently, the equilibrium constants for these reactions are available. Therefore, the method of treatment demonstrated here can be conveniently adopted to those processes which otherwise could not be modeled. Even if the homogeneous reactions may not be instantaneous, this treatment still could provide a reasonable approximation in many cases.

Acknowledgement

This work was sponsored by Great Lakes Chemical Corporation. We are grateful for the helpful discussions with Nick Macchiarolo and Jim Ayres who pointed out the importance of homogeneous equilibrium reactions in this system.

References

[1] Z. E. Jolles (Ed.), 'Bromine and its Compounds', Academic Press, New York (1966) pp. 27–9, p. 154, p. 747 and p. 750.
[2] D. S. Stasinevich, *Fiz.-Khim. Osn. Tekhnol. Pererab. Khim. Syr'ya* **2** (1976) 94.
[3] D. S. Stasinevich, *J. Appl. Chem. (USSR)* **51** (1978) 960.
[4] J. S. Newman and W. Tiedemann, *in* 'Advances in Electrochemistry and Electrochemical Engineering', Vol. 11, (edited by H. Gerischer and C. W. Tobias), John Wiley & Sons, New York (1978).
[5] J. A. Trainham and J. Newman, *J. Electrochem. Soc.* **124** (1977) 1528.
[6] J. M. Fenton and R. C. Alkire, *ibid.* **135** (1988) 2200.
[7] J. Newman and W. Tiedemann, *AIChE J.* **21** (1975) 25.
[8] D. S. Stasinevich and A. N. Usatov, *J. Anal. Chem. (USSR)* **33** (1978) 909.
[9] V. R. Gergert and Yu. F. Artamonov, *Zh. Neorg. Khim.* **21** (1976) 3160.
[10] Yu. F. Artamonov and V R. Gergert, *Russian J. Inorganic Chem.* **22** (1977) 8.
[11] D. S. Stasinevich, *J. Appl. Chem. (USSR)* **31** (1958) 694.
[12] *Idem, ibid.* **31** (1958) 833.
[13] D. S. Stasinevich and L. R. Berezovskii, *ibid.* **51** (1978) 611.

Appendix

Derivations of equilibrium relationships

Combining definitions of K_1 and K_3, one obtains

$$C_{Cl_2} = \frac{C_{Cl^-}}{K_1 K_3} \frac{C_{BrCl}}{C_{Br^-}} \tag{A1}$$

For HBrO, according to definitions of K_2 and K_3 gives

$$C_{HBrO} C_{H^+} = \frac{K_2 C_{BrCl}}{K_3 C_{Cl^-}} \tag{A2}$$

For HClO, using definition of K_7 gives

$$C_{HClO} C_{H^+} = K_7 \frac{C_{Cl_2}}{C_{Cl^-}} \tag{A3}$$

So, from Equations A1 to A3,

$$C_{HClO} = \frac{K_7}{K_1 K_2} \frac{C_{Cl^-}}{C_{Br^-}} C_{HBrO} \tag{A4}$$

Substituting C_{HClO} given above into Equation 20 and then combining with Equation A2 produces Equation 21.

Employing definitions of K_3 to K_8 gives, respectively,

$$C_{Br_2} = \frac{C_{BrCl} C_{Br^-}}{K_3 C_{Cl^-}} \tag{A5}$$

$$C_{BrCl_2^-} = K_4 C_{Cl^-} C_{BrCl} \tag{A6}$$

$$C_{Br_2Cl^-} = K_5 C_{Br_2} C_{Cl^-} \tag{A7}$$

$$C_{Br_3^-} = K_6 C_{Br^-} C_{Br_2} \tag{A8}$$

$$C_{Cl_3^-} = K_8 C_{Cl^-} C_{Cl_2} \tag{A9}$$

Substituting Equations A6 to A8 into Equation 22 gives

$$C_{Br^-} + 2C_{Br_2} + 3K_6 C_{Br^-} C_{Br_2} + C_{BrCl} + K_4 C_{Cl^-} C_{BrCl} + 2K_5 C_{Cl^-} C_{Br_2} = C_{Br}^0 - C_{HBrO} \tag{A10}$$

Replacing C_{Br_2} using Equation A5 yields Equation 23.

If ψ represents the C_{BrCl} obtained from Equation 23, then differentiating ψ with respect to C_{Br^-} is

$$\frac{dC_{BrCl}}{dC_{Br^-}} = \psi' \tag{A11}$$

Subsequently, differentiating Equations A1, A4, A6, and A9 produces

$$\frac{dC_{Cl_2}}{dC_{Br^-}} = \frac{C_{Cl^-}}{K_1 K_3 C_{Br^-}} \left[\psi' - \frac{\psi}{C_{Br^-}}\right] \tag{A12}$$

$$\frac{dC_{HClO}}{dC_{Br^-}} = \frac{K_7 C_{Cl^-}}{K_1 K_2} \left[\frac{1}{C_{Br^-}} \frac{dC_{HBrO}}{dC_{Br^-}} - \frac{C_{HBrO}}{(C_{Br^-})^2}\right] \tag{A13}$$

$$\frac{dC_{BrCl_2^-}}{dC_{Br^-}} = K_4 C_{Cl^-} \psi' \tag{A14}$$

$$\frac{dC_{Cl_3^-}}{dC_{Br^-}} = K_8 C_{Cl^-} \frac{dC_{Cl_2}}{dC_{Br^-}} \tag{A15}$$

The expressions for h_1, h_2, and h_3 (i.e. Equations 24 to 26) can be obtained using the above equations.